

Mechanics of the Dynamic Release Process for Stiction Failed Micro Cantilever Beams Using Structural Vibrations

Amit Savkar

Department of Mathematics
University of Connecticut, Storrs, CT 06269-3009, USA

Kevin D. Murphy

Department of Mechanical Engineering
University of Connecticut, Storrs, CT 06269-3139, USA

1. ABSTRACT

Recently it has been shown that structural vibrations are an efficient means to repair stiction failed microcantilever beams. Experiments and analysis have identified excitation parameters (amplitude and frequency) that successfully initiated the debonding process between the microcantilever and the substrate. That analysis could not describe what happened after the debonding process was initiated. For example it could not predict if the beam would transition from a s-shaped to an arc-shaped configuration or even be repaired to a free-standing beam. The current research examines the post-initiation behavior of stiction failed microcantilever beams. A new-coupled fracture/vibration model is formulated and used to track the evolution of the repair in order to determine the extent of repair under various conditions. This model successfully explains phenomenological observations made during the experiments regarding the repair process being dependent on direction of frequency sweeps, complete and partial repair, and monitors the degree of repair no repair, partial repair or complete repair along with releases time associated with such repairs.

2. INTRODUCTION

Recent studies conducted on microelectromechanical systems (MEMS) have suggested that sticking failure of individual components within a device is one of the most common and unavoidable reliability issue facing the industry.^{1,2} This particular failure mechanism, commonly referred to as stiction, is a significant roadblock preventing the widespread use of MEMS in commercial applications. Stiction failures, which are typically driven by surface forces, can be broken down into two categories. The first is fabrication failures. In this case, sticking contact is initiated as material is etched away and the device is *released*. The forces responsible for these failures include (but are not limited to) capillary forces, van der Waals forces, and electrostatic forces.³⁻⁵ The second type of failure occurs after the device is manufactured and has been put into use. These operational failures are referred to as *in-use* stiction. The mechanisms driving these failures are more diverse; dynamic effects may cause components to come into contact, where various forces may lead to adhesive contact. These include the surface forces listed previously, as well as Casimir forces, and Coulomb forces.^{1,6}

Research efforts aimed at improving device reliability at the fabrication stages have taken various tacks. These include introducing novel materials, thin film coatings, smart design changes, and post-fabrication manipulation. For example, during the fabrication of silicon molds for polymer optics, teflon-like material is used as a coating using a DRIE (deep reactive ion etching) process. This has been shown to reduce the stiction arising from chemical etching with KOH and IPA.⁷ Diamond like carbon coatings have been used to reduce the stiction properties of microspheres.⁸ And hydrogen elimination process have been developed for the removal of water molecules after the washing process.⁹ Shortly after fabrication (and before being put into operational use), laser pulse heating has been used to repair stiction failed micro-cantilevers.¹⁰⁻¹² This process directs a laser pulse at the failed component. The rapid expansion of the heated component produces thermal strains and causes

Further author information: (Send correspondence to K. D. Murphy)
e-mail: kdm@engr.uconn.edu, Telephone: +1 860 486 4109

Figure 1

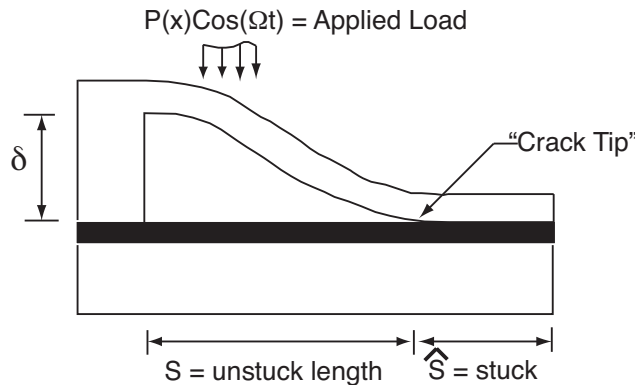


Figure 1: A schematic of a micro-cantilever stuck to a substrate. Its unstuck length is s . A periodic harmonic load is applied over a small portion of the beam, in an attempt to unstick it.

relative slip between the two mated surfaces, driving decohesion. Although this approach is very attractive, it is still inhibited by the fact the internal lattice heating can damage the component. This is particularly worrisome for those made out of polymeric and cellular materials, which appear in newer types of MEMS devices. Laser induced stress waves have also been considered, as a means to separate stiction failed MEMS structures.^{13,14} The latter two methods, while showing promise, require a good deal of hardware, set-up space, as well as easy access to the failed component. As a result, they are reasonable methods for fabrication failures but are considerably less attractive for repairing in-use devices.

For in-use stiction, research has focused on prevention - and not as much on repair. For example, consider RF MEMS switches. Common in-use failures modes include a trapped-charge mechanism¹⁵ and break down of the dielectric^{16,17}; material solutions for such problems have dominated. Self-assembled monolayers (SAM)¹⁸ have significantly reduced the release and in-use stiction, as compared to plasma deposited fluorocarbons. Designers have also proposed avoiding stiction by redesigns: by limiting the length of free standing cantilever beams stiction may be avoided during the operation of certain actuators.⁶ Additional features, such as sidewall spacers and bumps, may be etched into the device and help reduce the contact area of the neighboring surfaces, thereby reducing the potential for stiction.¹⁹ These design approaches have met with some success, though they limit design flexibility.

Recently, it has been shown that structural vibrations may be used as an effective alternative for the repair of stiction failed components.²⁰ The benefit to this approach is that electrical actuation pads may be built into the substrate of a MEMS chip and used to deliver a periodic electrical potential, driving the structural vibrations. In short, the built-in functionality of the chip may be used to effect the desired repair. The physical process behind this approach can be seen schematically in Figure 1. This shows a microcantilever stuck to a substrate. At the right end of the unstuck section, $x = s$, the beam and the substrate merge and form a singularity, which is geometrically similar to a crack tip. As the unstuck portion of the beam is driven, lateral vibrations are induced and the crack may or may not advance; the onset of crack propagation (also referred to as debonding or peeling, in this physical context) and its continued growth may be described via dynamic fracture mechanics. The preliminary work on this approach considered a beam with a fixed unstuck length, i.e. $s = \text{constant}$. Parameter combinations of the forcing amplitude and frequency (F, Ω) that *initiated* peeling were then obtained.²⁰ The present study differs in several ways - but the most dramatic difference is that the unstuck length is now a function of time, $s = s(t)$. As such, the evolution of the stiction repair process may be described. As an aside, it may be noted that because the domain of the problem is restricted to the unstuck portion of the beam (which changes with time), this problem constitutes a moving boundary problem.

The model developed here uses assumed modes (for spatial discretization) along with Lagrange's equations to

describe the lateral deformation of the unstuck portion, $w(x, t)$, and the growth of the unstuck portion, $s(t)$. This formulation incorporates inertial effects into Griffith's criterion for mode I fracture.^{22, 23} Finally, the limitations of this model should be clearly stated. This model may be used to examine growth of the unstuck region (i.e., crack growth). In other words, this model remains valid only for an advancing crack, $\dot{s} \geq 0$. The complex contact (and possibly re-adhesion) mechanics of crack closure are not considered here. A simple model for static crack closure has been proposed elsewhere.^{24, 25}

3. ANALYTICAL MODEL

The system under consideration is the s-shaped, stiction failed micro-cantilever, shown in "Fig. 1." The model will describe behavior only in the unstuck portion of the beam, $x \in [0, s]$. The beam is a homogeneous, linear Euler-Bernoulli beam with an unstuck length of s , total length of L , thickness h , and depth b . The left end is clamped and a distance δ above the substrate. The right end of the unstuck portion of the beam (at $x = s$) has a fixed displacement $w(s, t) = \delta$ and no slope. A distributed load is used to represent the electrical loading used in the preliminary experiments.²⁰ Of course, an electric lateral load will be gap dependent and, as the beam vibrates, this load will change. However, if the actuation pad used for exciting the beam is placed close to the left post (as in the experiments of reference²⁰), the lateral deflection will be small and the gap size will be roughly constant. Under these circumstances, the load may be expressed as

$$P(x, t) = P(x)[\cos(\Omega t) - 1]. \quad (1)$$

This consists of a static downward load and a periodic load. This excitation is consistent with the fact that upward forces are difficult to apply (note that the load never exceeds zero). In addition, the time-varying portion of this load gradually lifts off from zero (with zero slope at $t = 0$), as would most realistic loadings.

The total lateral beam deflection $w(x, t)$ is measured from the free-standing configuration and consists of two parts. The first represents the no-load equilibrium position of the adhered beam, i.e., describing the s-shape. This deflection is given by $w_s(x, t)$ and may be obtained by elementary beam theory with the boundary conditions: $w_s(0, t) = 0$, $w'_s(0, t) = 0$, $w_s(s, t) = \delta$, and $w'_s(s, t) = 0$, where primes denote differentiation with respect to x . The result is

$$w_s(x, t) = \delta \left[\frac{3x^2}{s(t)^2} - \frac{2x^3}{s(t)^3} \right], \quad (2)$$

which will clearly evolve as the beam unpeels from the substrate and $s(t)$ increases. The second part of the lateral deformation is produced by the applied load, "Eq.(1)". This represents the lateral vibration of the unstuck portion of the beam and is given by $w_m(x, t)$ (the subscript m denotes *mode*). These vibrations occur about the s-shape, $w_s(x, t)$. And because the problem is linearly elastic and superposition holds, the total deformation is simply $w(x, t) = w_s(x, t) + w_m(x, t)$. From this description of the total deformation, it is evident that the shape w_m must satisfy clamped-clamped boundary conditions at $x = 0$ and $x = s$. Assuming the response is dominated by a single mode, the vibration response may be expressed as

$$w_m(x, t) = A(t)\Psi_1 \left(\frac{x}{s(t)} \right). \quad (3)$$

Here, A is the time dependent first mode amplitude and Ψ_1 is the time dependent first clamped-clamped vibration mode shape. This problem has two generalized coordinates $s(t)$ and the modal amplitude $A(t)$. Lagrange's equations are used to obtain the equations that govern the behavior of s and A . The details of this analytical formulation is given in reference.²¹ The analysis produces two coupled nonlinear ODE's in the unknowns s and A and are given as:

$$(C_1 + C_2A^2 + C_3\delta A)\ddot{s} + (C_4A - C_5)\ddot{A} = (\kappa_1 + \kappa_2 + \kappa_3 + \kappa_4 + Q_s), \quad (4)$$

where

$$\kappa_1 = C_5 \dot{A}^2 \quad (5a)$$

$$\kappa_2 = (C_7 A^2 + C_8 A + C_9) \frac{\dot{s}^2}{s} \quad (5b)$$

$$\kappa_3 = -(C_{10} A + C_{11}) \frac{\dot{A} \dot{s}}{s} \quad (5c)$$

$$\kappa_4 = \frac{P_1 A}{s^4} + \frac{P_2}{s^4} + \frac{P_3 A^3}{s^4} \quad (5d)$$

and

$$(P_4 A - P_5) \ddot{s} + P_6 s \ddot{A} = (\varphi_1 + \varphi_2 + \varphi_3 + Q_A), \quad (6)$$

where

$$\varphi_1 = (P_7 A - P_8) \frac{\dot{s}^2}{s} \quad (7a)$$

$$\varphi_2 = (P_9) \dot{A} \dot{s} \quad (7b)$$

$$\varphi_3 = \frac{-P_{10} A}{s^3} - \frac{P_{11}}{s^3} \quad (7c)$$

where $C_1 \rightarrow C_{11}$, and $P_1 \rightarrow P_{11}$, are constants which arise out of the analysis. The values of these constants have been provided in the appendix C.²¹

4. NUMERICAL FORMULATION

A traditional time marching approach is used to obtain a solution to the governing equations. This requires that the equations be re-cast first order form; this converts the two, second order equations into four, first order ODE's in the variables A , \dot{A} , s , and \dot{s} . Once in this form, a simple fourth order Rung-Kutta was used.²⁸ Throughout every simulation, the sign of \dot{s} was constantly monitored; if $\dot{s} < 0$, the model would no longer be valid and the simulation was stopped.

5. RESULTS

In this section we shall consider the various different response characteristic such as the influence of harmonic loading on the system, the importance of lateral vibrations, the effect of force and frequency on the repair process of the unstuck beam etc. First the importance of the lateral vibrations ($A(t)$) is highlighted. Next the effect of force on different unstuck length is studied and role of frequency on repair process is examined. Finally frequency sweep is carried to confirm certain behavior seen experimentally.²⁰

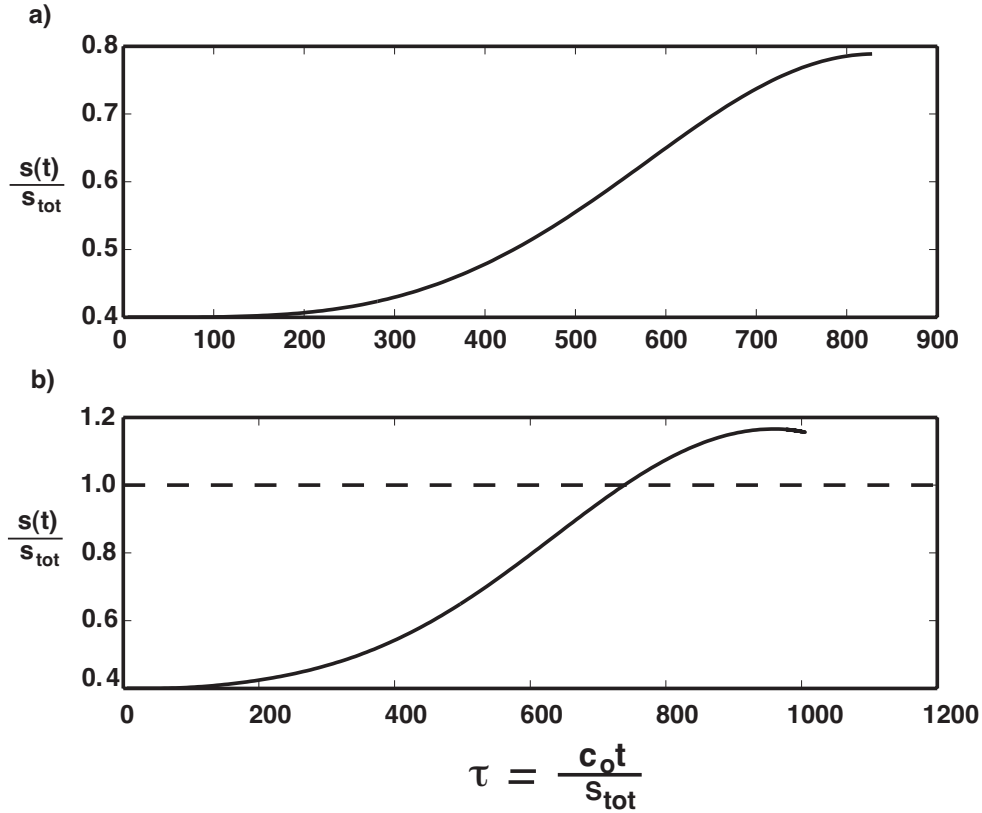


Figure 2: A plot of non dimensional beam length versus non dimensional time showing the effect of modal amplitude for a fixed force value. $s_o = 600\mu m$, $s_{tot} = 1500\mu m$.

5.1. Harmonic excitation

The final objective is to characterize the growth of the unstuck region under periodic loading. In other words we are interested in $s(t)$ the longitudinal length of the unstuck beam. This leaves us with the question whether lateral vibrations is important in this context. Moreover in the traditional cantilever dynamic fracture literature (with static loads), lateral vibrations are uniformly neglected.²² To understand this, two different simulations were carried out. In the first case Equation 4 and Equation 6 were simultaneously integrated, with the modal amplitude and its derivatives set to zero, such that lateral amplitude were completely ignored. The second case does not put any restrictions on the modal amplitude or its derivatives thus incorporating w_m in the response. The beams have a elastic modulus of $160GPA$, width is $30\mu m$, and thickness $2\mu m$. The force amplitude was $P = 1500\mu N$, and the excitation frequency was $\Omega/\omega_1 = 0.9$, where ω_1 is the first natural frequency of the beam in initial shape.

“Figure 2”, shows the growth of the unstuck region for these two cases. The first case (2a) shows that the stuck beam unpeels to a final length of approximately $s/s_{tot} = 0.78$ before it arrests. It means that the result was a partial repair. The second case (2b) shows that the length grows to approximately $s/s_{tot} = 1.1$ before it arrests. The dotted line in the “Figure (2b)” shows the cut of length or the total length of the beam. Any curve beyond this horizontal line does not carry any physical meaning. Thus by this simple case it can be concluded that lateral amplitude can have a tremendous impact on the extent of repair and should not be ignored.

5.2. Force amplitude and excitation frequency

In reference,²⁰ it was shown that the forcing amplitude and frequency dramatically influenced whether the debonding process was initiated or not. In that study, it was shown that if the excitation frequency was near a

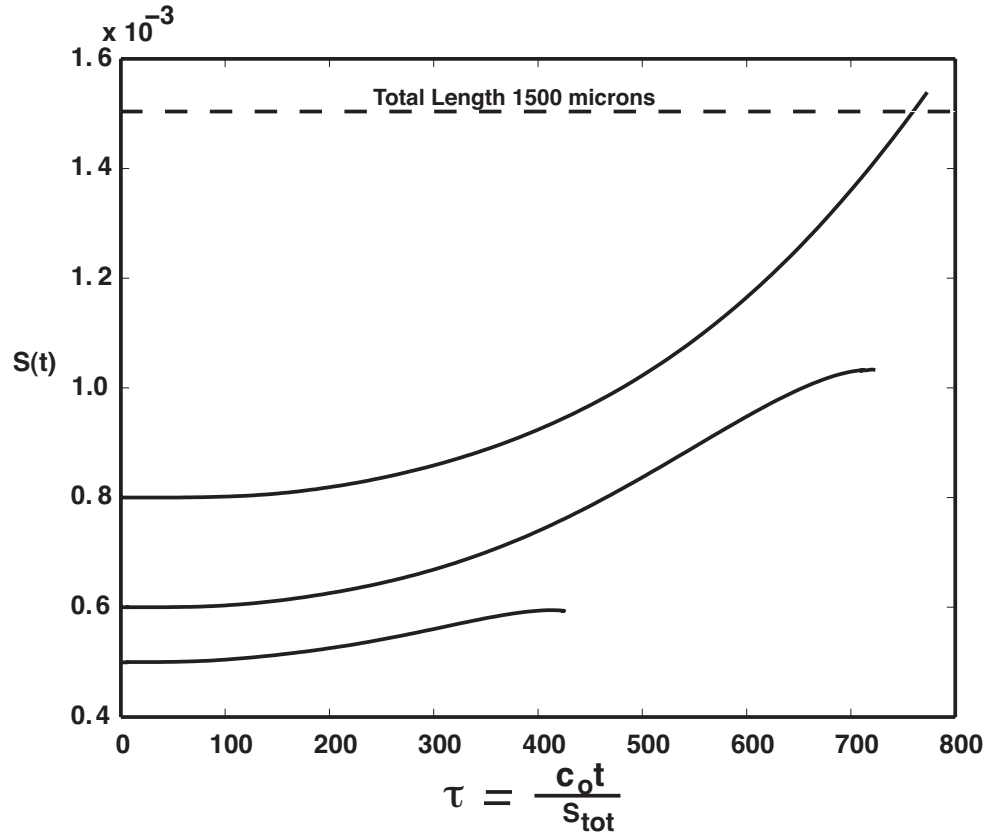


Figure 3: A plot of various unstuck beam length versus non dimensional time showing the effect of fixed force and excitation frequency on various initial unstuck lengths . $s_o = 500\mu m, 600\mu m, 800\mu m, s_{tot} = 1500\mu m$.

resonant frequency, debond initiation was much more likely. Likewise, it is important to see how these quantities impact the debonding process after initiation.

The material properties and beam geometry are the same as in the previous case. To examine the impact of the excitation amplitude only, the excitation frequency is held fixed at $\Omega/\omega_1 = 0.9$, where ω_1 is the first natural frequency of the system at its initial unstuck length, s_o . However, it should be noted that this is *not truly* a fixed frequency problem. As the unstuck region grows, the effective length of the beam (i.e., its free length) grows, which reduces the natural frequency. So even though the driving frequency Ω is fixed, its proximity to the resonance condition changes. But a fixed Ω is physically easy to realize and, hence, of practical importance.

“Figure. 3,” shows the growth of the unstuck region as a function of time for various initial unstuck lengths. These show a monotonic increase in the final unstuck length as the initial unstuck length changes. As such one can see that at a given forcing amplitude and the excitation frequency as the initial unstuck length increases, the extent of repair also increases. It means that to obtain a higher repair for a beam with a 33.33% unstuck length more force will be required to obtain the same repair as a beam which, has 40% unstuck length.

Now consider the impact of the excitation frequency. Here the same physical system is used and the excitation amplitude is fixed at $P = 1500\mu N$. “Figure. 4 ,” shows how the unstuck region grows as a function of time. If the excitation frequency is $\Omega = 0.5\omega_1$, the beam is repaired. If the excitation frequency is increased still further to $\Omega = 0.75\omega_1$, the unstuck length grows to $0.75s_{tot}$ and then arrests, short of full repair. If the excitation frequency is further increased to near resonance $\Omega = 0.9\omega_1$ the extent of repair drops to $0.65s_{tot}$. This result may seem unusual. Driving the system closer to (the initial) resonance actually produces less repair than driving it at half of the (initial) resonance. This may be explained as follows. For $\Omega = 0.9\omega_1$, the excitation is initially

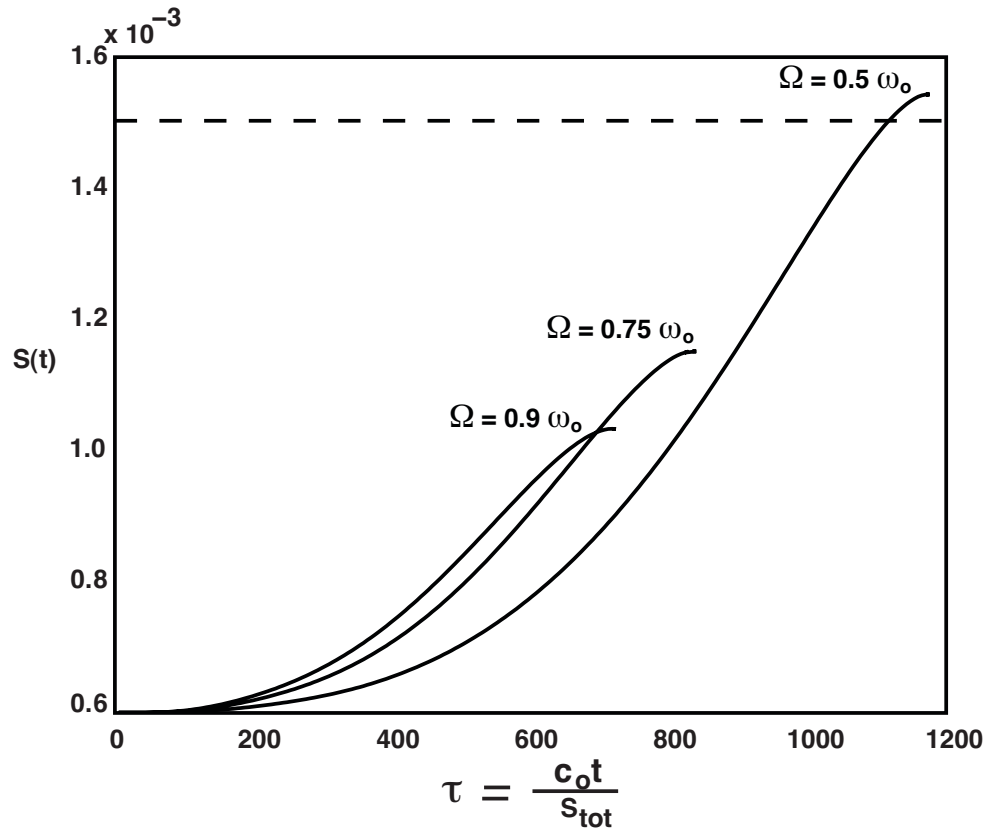


Figure 4: .A plot of non dimensional beam length versus non dimensional time showing the effect of variation of excitation frequency for a fixed force value $s_o = 600\mu m$, $s_{tot} = 1500\mu m$.

sub-resonant (though nearly resonant) and debonding begins immediately with a large velocity. However, as the beam unsticks, the natural frequency drops and passes through the excitation frequency. The excitation frequency very quickly becomes super-resonant ($\Omega \gg \omega_1$), reducing the steady-state vibration amplitude. This causes the system to arrest. But, for the case $\Omega = 0.5\omega_1$, the situation is different. Debonding is initiated and, again, the natural frequency drops. But it takes longer for the natural frequency to coincide with the excitation frequency. This permits more momentum to build, such that the debonding process may be carried through to completion.

5.3. Frequency sweep

Frequency sweeps refers to increasing or decreasing the excitation frequency at a prescribed rate. Preliminary experiments have used frequency sweeps and shown that the extent of a repair depends on the direction of the sweep.²⁰ This directional dependence could not be explained previously as the model only looked at the parameters that *initiated* stick release. The current analytical model is capable of capturing this phenomenon and explaining the underlying physics of such an occurrence. “Figure. 5,” shows two curves. The first curve indicates the length of the unstuck beam when the excitation frequency is swept up. Here the frequency was swept up over the range, $0.1\omega_1 \rightarrow \Omega \rightarrow 1.5\omega_1$, where ω_1 is the first natural frequency of the beam for $s = s_o$. The sweep rate was set at $\Delta\Omega = 10$ Hz. This is achieved by incrementing the excitation frequency during each time step by a fixed amount keeping the force at a constant value. The second curve indicates the length of the unstuck beam when the excitation frequency is swept down: $1.5\omega_1 \rightarrow \Omega \rightarrow 0.1\omega_1$. Again the sweep rate was set to $\Delta\Omega = 10$ Hz. It is observed that sweeping the excitation frequency down produces complete repair while sweeping up only repairs the beam partially. This phenomenon is exactly the same as was observed in the preliminary experiments.²⁰

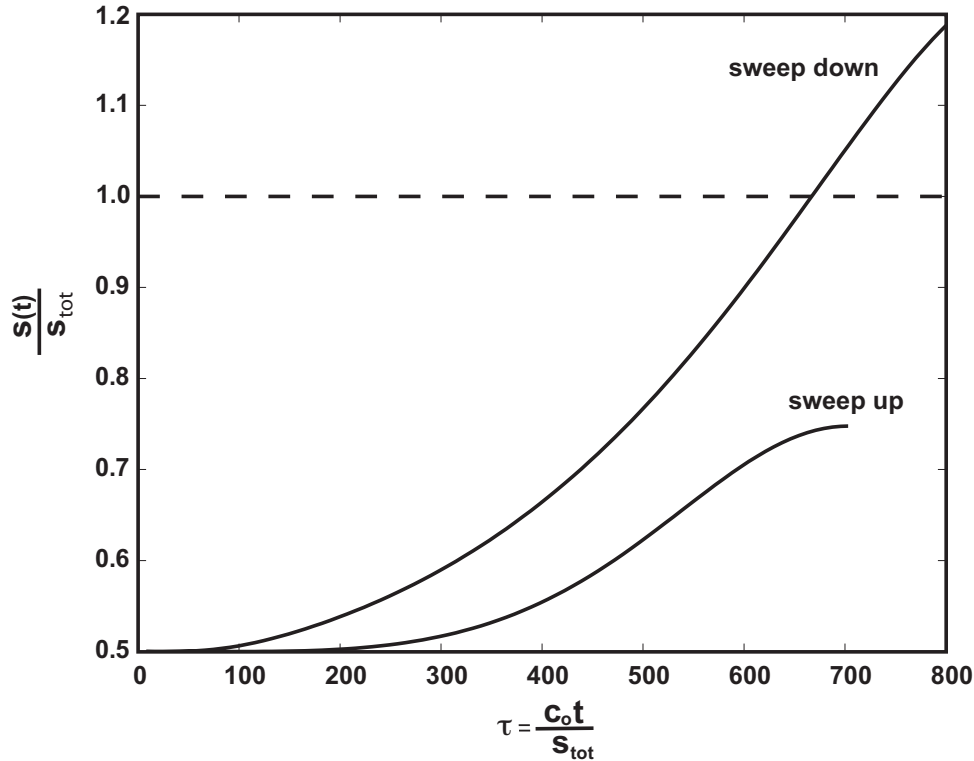


Figure 5: A plot of non dimensional beam length versus non dimensional time showing the effect of frequency sweep up and down for a fixed force value . $s_o = 700\mu m$, $s_{tot} = 1400\mu m$.

This behavior can be explained by understanding the shift in the first fundamental frequency ω_1 of the unstuck beam. As the beam begins to peel off $s(t)$ increases, and ω_1 begins to drop. As the excitation frequency is also decreased in the sweep down, bringing the excitation frequency Ω in closer proximity to ω_1 . In a sense, the excitation chases the resonant frequency encouraging resonance and promoting repair. When the excitation frequency is swept up from $\Omega = 1.5\omega_1$ to $\Omega = 0.1\omega_1$ the excitation frequency increases while the natural frequency decreases. They quickly pass through one another and continue to move apart, preventing a continued near resonant condition and hindering the repair. It can be concluded that sweeping the excitation frequency down is more effective [i.e., if down sweeps promote a more complete repair] than frequency sweep up.

6. CONCLUSIONS

This paper explores the underlying physics of post initiation stiction release phenomenon. An analytical modal which is a combination of vibration and dynamic fracture mechanics has been developed successfully. The numerical simulations performed help in establishing the importance of lateral vibrations, effect of forcing amplitudes and excitation frequency. It also provides an insight to the experimental results as seen in.²⁰

REFERENCES

1. W. Merlijn van Spengen, MEMS reliability from a failure mechanisms perspective *Microelectronics Reliability* 43(7) 2003 1049 - 1060.
2. W. Merlijn Van Spengen, R. Puers and I. De Wolf, A physical model to predict stiction in MEMS *Journal of Micromechanics and Microengineering* 12 2002 702 - 713.

3. C.H. Mastrangelo, C.H. Hsu, Mechanical stability and adhesion of microstructures under capillary forces. Part I. Basic theory *Journal of Microelectromechanical Systems* 2 (1993) 33 - 43.
4. C.H. Mastrangelo, C.H. Hsu, Mechanical stability and adhesion of microstructures under capillary forces. Part II. experiments *Journal of Microelectromechanical Systems* 2 (1993) 44 - 55.
5. M.P. de Boer, J. A. Knapp, T.A. Michalske, U. Srinivasan, R. Maboudian, Adhesion hysteresis of silicane coated microcantilevers *Acta Materialia* 48 2000 4531 - 4541.
6. R. W. Johnstone and M Parameswaran, Theoretical limits on the freestanding length of cantilevers produced by surface micromachining technology *Journal of Micromechanics and Microengineering* 12 2002 855 - 861.
7. D. Nilsson, S. Jensen, and A. Menon, Fabrication of silicon molds for polymer optics *Journal of Micromechanics and Microengineering* 13 2003 S57 - S61.
8. W.R. Ashurst, C. Yau, C. Carraro, C. Lee, G.J. Kluth, T.R. Howe, R. Maboudian, Alkene based monolayer films as anti-stiction coatings for polysilicon MEMS *Sensors and Actuators A: Physical*, 91 (3) 2001 239-248.
9. N. Fujitsuka, and J. Sakata, A new processing technique to prevent stiction using silicon selective etching for SOI-MEMS, *Sensors and Actuators A: Physical* 97-98 2002 716 - 719.
10. N.C. Tien, S. Jeong, L.M. Phinney, K. Fushinobu, J. Bokor, Surface adhesion reduction in silicon microstructures using femtosecond laser pulses *Applied Physics Letters* 66(2) 1995 197 - 199.
11. K. Fushinobu, L.M. Phinney, N.C. Tien, Ultrashort-pulse laser heating of silicon to reduce microstructure adhesion *International Journal of Heat and Mass Transfer* 39(15) 1996 3181 - 3186.
12. L.M. Phinney, J.W. Rogers, Pulsed laser repair of adhered surface -micromachined polycrystalline silicon cantilevers *Journal of Adhesion Science and Technology* 17(4) 2003 603-622.
13. V. Gupta, R. Snow, M. . Wu, A. Jain, and J. Tsai, Recovery of stiction-failed MEMS structures using laser induced stress waves *Journal of Microelectromechanical Systems* 13(4) 2004 696 - 700.
14. Z.C. Leseman, S. Koppaka, and T.J. Mackin, A fracture mechanics description of stress wave repair in stiction-failed microcantilevers: theory and experiments *Journal of Microelectromechanical Systems* in press, 2007.
15. M. P. de Boer, D. L. Luck, W. R. Ashurst, R. Maboudian, A. D. Corwin, J. A. Walraven, and J. M. Redmond, High performance surface micromachined inchworm actuator *Journal of Microelectromechanical Systems* 13 (1) 2004 63 - 74.
16. W. Merlijn Van Spengen, R. Puers R. Mertens, and I. De Wolf, A low frequency electrical test set-up for the reliability assessment of capacitive RF MEMS switches *Journal of Micromechanics and Microengineering* 13 2003 604 - 612.
17. D. Dubuc, M. Saddaoui, S. Melle, F. Flourens, L. Rabbia, B. Ducarouge, K. Grenier, P. Pons, A. Boukabache, L. Bary, A. Takacs, H. Aubert, O. Vendier, J. L. Roux, and R. Plana, Smart MEMS concept for high secure RF and millimeterwave communications *Microelectronics Reliability* 44 2004 899 - 907.

18. U. Srinivasan, M. R. Houston, R. T. Howe and R. Maboudian, Alkyltrichlorosilane-based self assembled monolayer films for stiction reduction in silicon micromachines *Journal of Microelectromechanical Systems* 7 (2) 1998 252 - 260.
19. N. Tas, T. Sonnenberg, H. Jansen, R. Legtenberg, M. Elwenspoek, Stiction in surface micromachining *Journal of Micromechanics and Microengineering* 6 1996 385 - 397.
20. A.A. Savkar, K.D. Murphy, Z.C. Leseman, T.J. Mackin and M.R. Begley, On the use of structural vibrations to release stiction failed MEMS *Journal of Microelectromechanical Systems* 16 (1) 2007 163-173.
21. A.A. Savkar, *A Study of Stiction Repair in Micro-Cantilevers Using Structural Vibrations*, Ph.D. Thesis, The University of Connecticut, Storrs, CT. 2007
22. L.B. Freund, *Dynamic Fracture Mechanics*, Cambridge, Cambridge University Press, 1990.
23. J. P. Berry, Some kinetic consideration of the Griffith criterion for fracture-I, Equation of motion at constant force *Journal of Mechanics and Physics of Solids* 8 1960 194 - 206.
24. M. F. Kanninen, An augmented double cantilever beam model for studying crack propagation and arrest *International Journal of Fracture* 9 (1) 1973 83 - 91.
25. M. F. Kanninen, A dynamic analysis of unstable crack propagation and arrest in DCB test specimen *International Journal of Fracture* 10 (3) 1974 415 - 430.
26. C. T. Chang and R. C. Craig, Normal modes of uniform beams, *Journal of Engineering Mechanics Division. ASCE* 1969 1027-1031.
27. W. D. Zhu and J. Ni, Energetics and stability of translating media with an arbitrary varying length *Journal of Vibration and Acoustics* 122 2000 295 -304.
28. W.H. Press, W.T. Vetterling, S.A. Teukolsky, B.P. Flannery, *Numerical Recipes in Fortran The Art of Scientific Computing* Cambridge University Press, NewYork , 1994.